A Mitochondrial Protease with Two Catalytic Subunits of Nonoverlapping Specificities

Jodi Nunnari, Thomas D. Fox, Peter Walter

The mitochondrial inner membrane protease is required for the maturation of mitochondrial proteins that are delivered to the intermembrane space. In the yeast *Saccharomyces cerevisiae*, this protease is now shown to be a complex that contains two catalytic subunits, Imp2p and the previously identified Imp1p. Primary structure similarity indicates that Imp1p and Imp2p are related to each other and to the family of eubacterial and eukaryotic signal peptidases. Imp1p and Imp2p have separate, nonoverlapping substrate specificities. In addition to its catalyzing the cleavage of intermembrane space sorting signals, Imp2p is required for the stable and functional expression of Imp1p. Thus, inner membrane protease, and by analogy eukaryotic multisubunit signal peptidases, may have acquired multiple catalytic subunits by gene duplication to broaden their range of substrate specificity.

Nuclear-encoded mitochondrial proteins that are targeted to the intermembrane space (IMS), such as cytochrome c_1 and cytochrome b_2, are synthesized as precursors by cytosolic ribosomes. Both pre–cytochrome c_1 and pre–cytochrome b_2 contain bipartite signal sequences that are processed in two sequential proteolytic steps in distinct mitochondrial compartments (*1–6*). The most amino-terminal part of the signal sequence is a signal that is responsible for targeting the proteins to mitochondria and initiating import into the matrix compartment. Matrix targeting signals have the properties of positively charged, strongly amphipathic α helices. During import, the IMS precursor proteins become at least partially exposed to the matrix space, where the matrix targeting portion of the signal sequence is removed by a soluble metalloprotease, a protein complex consisting of two related subunits, Mas1p and Mas2p (*7–9*). The second part of the signal sequence is a targeting signal required for localization of the intermediate forms of the proteins (i-cytochrome c_1 and i-cytochrome b_2) to the IMS (*10, 11*).

The mechanism by which the IMS signal targets these proteins to the IMS is still unclear. According to the stop transfer model, it mediates the direct import of the protein into the IMS across the outer membrane (*10–13*). Although translocation into the matrix space is initiated by the preceding matrix signal, the IMS signal would function as a stop-transfer domain that prevents protein translocation across the inner membrane. According to an alternative view, the conservative sorting model, the IMS targeting signal functions to direct to the IMS the export of proteins that have been fully imported across the inner membrane into the matrix (*14, 15*). In this case, the IMS signal would function like bacterial signal sequences, which direct the export of preproteins from the cytoplasm into the periplasmic space. At present, there is experimental evidence consistent with both proposed mechanisms (*13, 15, 16*).

Although most mitochondrial proteins are encoded by nuclear genes, the mitochondrial genome of *S. cerevisiae* encodes a small subset of its own proteins. One of these proteins is the integral membrane protein cytochrome oxidase subunit II (COXII), a component of the inner membrane cytochrome oxidase complex. The COXII is synthesized as a precursor (pre-COXII) by mitochondrial ribosomes that are, presumably, membrane bound, and is integrated co-translationally into the inner mitochondrial membrane (*17, 18*). The integration leads to the translocation of a large part of pre-COXII across the membrane into the IMS, where the pre-sequence is cleaved to produce mature COXII (*18, 19*).

To lend insight into the mechanism of maturation of IMS proteins, we examined the question of whether the maturation pathways of proteins that originate in two distinct compartments, the mitochondrial matrix and the cytoplasm, converge at common components. One known component that affects the maturation of both the mitochondrial-encoded pre-COXII and the nuclear-encoded cytochrome b_2 is the inner membrane protease I (Imp1p). The Imp1p is associated with the intermembrane face of the inner membrane and is required for the processing of the IMS signal from both pre-COXII and i-cytochrome b_2 (*20–22*). On the basis of sequence comparisons, Imp1p is a member of the signal peptidase family, a group of eubacterial and eukaryotic membrane-bound endoproteases that function to cleave secretory signal sequences (*22*). Indeed, IMS sorting signals are composed of a stretch of hydrophobic amino acids flanked by charged residues and, therefore, closely resemble secretion signals, indicating that these related proteases also share the structural features required for the recognition of such signal sequences (*8, 23, 24*). The processing of the IMS sorting signal of cytochrome c_1 does not require Imp1p, however, indicating that a second IMS protease must exist (*20, 22*).

We chose a genetic approach to further examine the maturation pathways of IMS proteins. Our initial strategy entailed a screen for mutants that cause the accumulation of pre-COXII, which were subsequently screened for effects on cytochrome b_2 and cytochrome c_1. The screen was designed to identify novel gene products that function at a point after convergence of the biosynthetic pathways of mitochondrial-encoded and nuclear-encoded IMS proteins.

Accumulation of precursor and intermediate forms of IMS proteins in mutant cells. For the isolation of *S. cerevisiae* mutants with specific defects in the synthesis or processing of mitochondrial-encoded proteins, we screened a bank of nonrespiring mutants (pet^- mutants) by labeling cells with [^{35}S]methionine in the presence of cycloheximide (*25*). This drug inhibits cytosolic, but not mitochondrial, protein synthesis. Separation of the translation products by SDS–polyacrylamide gel electrophoresis (PAGE) revealed a simple pattern of bands in which individual mitochondrial proteins were easily distinguishable. From this screen, we isolated a mutant strain termed MKK212 in which the synthesis of all mitochondrial-encoded proteins was normal, but COXII accumulated as a precursor (pre-COXII) (Fig. 1 and Table 1). This strain was characterized by backcrossing to the congenic wild-type strain DL2 (*26*), and monitoring the mitochondrial protein synthesis of the meiotic products (Fig. 1). A slower migrating band corresponding to pre-COXII accumulated in two of the four meiotic products (Fig. 1, lanes 2 and 4) derived from a single tetrad. This mutant phenotype co-segregated with the pet^- phenotype, scored by the ability to grow on the nonfermentable carbon sources ethanol and glycerol (Fig. 1). These results suggest that the accumulation of pre-COXII

J. Nunnari and P. Walter are in the Department of Biochemistry and Biophysics, University of California Medical School, San Francisco, CA 94143–0448. T. D. Fox is in the Section of Genetics and Development, Cornell University, Ithaca, NY 14853–2703.

resulted from a single nuclear mutation that impeded respiration. All further experiments described below were performed with mutant strain JN109, which was derived from this backcross.

To determine whether the mutation in JN109 cells also affected the maturation of nuclear-encoded mitochondrial proteins, we monitored the fate of several newly synthesized nuclear-encoded proteins. To this end, wild-type DL2 cells and mutant JN109 cells were labeled with [^{35}S]methionine. Nuclear-encoded mitochondrial proteins were immunoprecipitated from the labeled cell extract and analyzed by SDS-PAGE. Mutant JN109 cells specifically accumulated the intermediate forms of two nuclear-encoded IMS proteins, cytochrome b_2 (Fig. 2B, lane 4, i-cytochrome b_2) and cytochrome c_1 (Fig. 2C, lane 4, i-cytochrome c_1). For both cytochromes, the intermediate forms migrated between the mature (Fig. 2, B and C, lanes 2) and precursor (Fig. 2, B and C, lane 1) forms, indicating that the matrix targeting, but not the IMS targeting signal was removed. In contrast, the import and processing of the matrix protein $F_1\beta$-adenosine triphosphatase was unaffected by the mutation in JN109 cells (Fig. 2A, lane 4). Taken together, these data show that the mutation in JN109 cells does not affect processing of the matrix targeting signal by the Mas1p-Mas2p protease complex of nuclear-encoded matrix or IMS proteins, but blocks the processing of the IMS targeting signal.

The mitochondrial inner membrane protease I (Imp1p) is required for the processing of pre-COXII and i-cytochrome b_2 (*20–22*) (Fig. 2B, lane 3). As previously observed, *imp1* mutant cells were shown to process i-cytochrome c_1 normally, suggesting that the mutation in JN109 cells resides at a locus other than *IMP1* (*20–22*) (Fig. 2C, lane 3). A diploid strain resulting from a cross of MKK148(*imp1-1*) and JN109 cells was not defective in the processing of IMS proteins, indicating that the two mutants belong to different complementation groups (*27*). The broader spectrum of IMS proteins affected in JN109 cells—as compared to the more limited spectrum of IMS proteins affected in MKK148(*imp1-1*) cells—suggests that the gene mutated in JN109 cells encodes a component that precedes processing by Imp1p in the maturation pathway of IMS proteins or that is directly required for Imp1p function.

Localization of intermediate forms of nuclear-encoded IMS proteins in the IMS. Two different defects could account for the accumulation of pre-COXII, i-cytochrome b_2, and i-cytochrome c_1 in mutant JN109 cells. First, the mutant gene may encode a component essential for the translocation of both nuclear-encoded IMS proteins and mitochondrial-encoded COXII across the inner mitochondrial membrane. Such a component might be a part of the putative re-export machinery, proposed to exist in the conservative sorting model for nuclear-encoded IMS proteins. If so, the intermediate forms of the IMS proteins would be expected to accumulate in the matrix space of the mitochondria. A second possibility is that the mutant gene encodes a component that is essential for the maturation of IMS proteins and is required for their correct folding, assembly, modification, or processing (or any combination thereof). In this case, i-cytochrome b_2, i-cytochrome c_1, and pre-COXII would be expected to be exposed to the IMS.

To distinguish between these possibilities, we determined the sub-mitochondrial location of i-cytochrome b_2 and i-cytochrome c_1 in JN109 cells. Mitochondria from both wild-type DL2 and JN109 cells were isolated and converted to mitoplasts by selective rupture of the outer membrane by hypo-osmotic shock. This treatment of mitochondria isolated from wild-type DL2 cells caused the release of the soluble IMS protein cytochrome b_2, which, after centrifugation, was recovered primarily in the supernatant fraction (Fig. 3A, lanes 1 and 5). Cytochrome c_1 remained associated with the mitoplasts and after centrifugation was recovered in the pellet (Fig. 3A, lanes 6). Although mature cytochrome c_1 is anchored

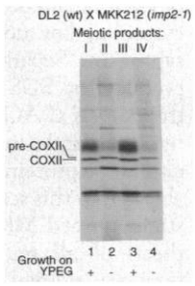

Fig. 1. A nuclear mutation in strain MKK212 causing a precursor form of mitochondrial-encoded cytochrome oxidase II to accumulate. Mitochondrial translation products were monitored in the four meiotic products resulting from a cross between DL2(wt) and MKK212(*imp2-1*) by [^{35}S]methionine labeling in the presence of cycloheximide. Cultures were grown at 30°C to 2 units (A_{600}) per milliliter in YP medium containing 2 percent galactose (*51*). The cells were labeled with 50 μCi of [^{35}S]methionine per A_{600} unit in the presence of cycloheximide (at 1 mg/ml) for 15 minutes. Mitochondria were prepared from the labeled cells by bead beating and centrifugation at 10000*g* for 10 minutes and analysis by SDS-PAGE and autoradiography. Incorporation of [^{35}S]methionine into mitochondrial translation products was variable between experiments. The growth phenotype of each of the meiotic products on YP plates containing ethanol and glycerol, YPEG, as indicated by (+) or (−).

Table 1. Yeast strains.

Strain	Genotype	Reference
MKK212	*ade2; ino4-8; ino1-13; imp2-1; Matα*	This study
MKK148	*ade2; ino4-8; ino1-13; imp1-1; Matα*	(*27*)
JN109	*ade2; lys2; imp2-1; Matα*	This study
DL2	*lys2; Mata*	(*26*)
PS32.3C	*ade2; his3-Δ200; leu2-3,112; ura3-52; Mata*	(*61*)
JN143	*ade2; his3-Δ200; leu2-3,112; ura3-52; imp2-1; Mata*	This study
W303-1B	*ade2-1; leu2-3; his3-11,−15; trp1-1; ura3-1; can1-100; Matα*	(*62*)
JN174	same as W303-1B, except *imp2::LEU2*	This study

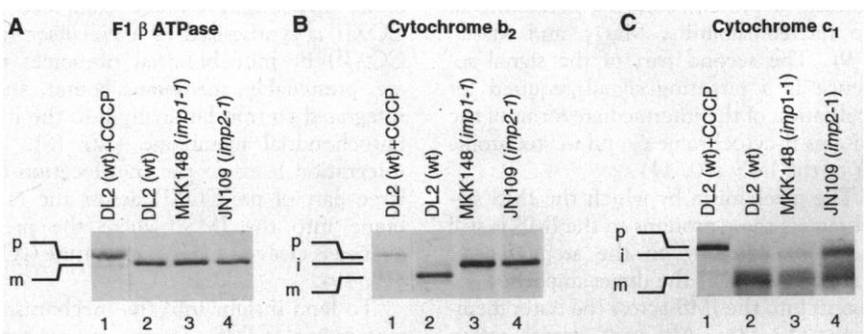

Fig. 2. Accumulation of intermediate forms of nuclear-encoded mitochondrial IMS proteins in JN109 cells. DL2(wt), MKK148 (*imp1-1*) or JN109 (*imp2-1*), cells were grown YP medium containing 2 percent galactose to log phase at 30°C and were labeled for 10 minutes with [^{35}S]methionine (50 μCi of [^{35}S]methionine per A_{600} unit). Immunoprecipitations were performed after SDS-denaturation of the cell extracts with antibodies to the proteins indicated (*52*). Precursor forms were accumulated by labeling DL2 cells in the presence of the uncoupler carbonyl cyanide *m*-chlorophenylhydrozone (CCCP; Sigma), a compound that collapses the electrochemical gradient across the inner mitochondrial membrane. (**A**) The mature (m) and precursor (p) forms of $F_1\beta$-ATPase are indicated. (**B**) The precursor (p), intermediate (i), and mature (m) forms of cytochrome b_2, and cytochrome c_1 (**C**) are indicated.

to the inner membrane with a large hydrophilic domain exposed in the IMS, it was resistant to proteolysis in mitoplasts isolated from wild-type cells (Fig. 3A, lanes 7 and 8), most likely because of its compact folding and tight association with other components in the cytochrome bc_1 complex (*28, 29*). The soluble matrix protein α-ketoglutarate dehydrogenase (KDH)—chosen as a control because of its exquisite sensitivity to proteolysis (*13*)—was protected from digestion by proteinase K in both intact mitochondria (Fig. 3A, lanes 3 and 4) and mitoplasts (Fig. 3A, lanes 7 and 8), indicating that the inner membrane remained intact under our experimental conditions.

In contrast to the mature cytochrome b_2 in mitochondria from wild-type cells, most of the i-cytochrome b_2 accumulating in mitochondria from JN109 mutant cells remained associated with mitoplasts (Fig. 3B, lane 6). To discriminate whether the mitoplast-associated i-cytochrome b_2 was localized entirely in the matrix space or was exposed to the IMS while still being associated with the inner membrane, we treated the mitoplasts with protease. We found that i-cytochrome b_2 was susceptible to proteolysis in mitoplasts (Fig. 3B, lanes 7 and 8), but not in intact mitochondria (Fig. 3B, lanes 3 and 4). Similarly, protease treatment of mitoplasts from JN109 cells resulted in the complete degradation of i-cytochrome c_1, indicating that the i-cytochrome c_1, like i-cytochrome b_2, was exposed to the IMS (Fig. 3B, lanes 7 and 8). The protease sensitivity of i-cytochrome c_1 in mitoplasts from mutant JN109 cells, in contrast to the resistance of mature cytochrome c_1 to proteolysis in wild-type cells, suggests that i-cytochrome c_1 may not be as compactly folded or assembled into the cytochrome bc_1 complex as mature cytochrome c_1. The control matrix protein, KDH, was protected from proteolysis in mitoplasts isolated from JN109 cells, indicating that the inner membrane was intact (Fig. 3B, lanes 7 and 8) in mitoplasts isolated from the mutant cells. Taken together, these data suggest that both i-cytochrome b_2 and i-cytochrome c_1 in JN109 cells are associated with the inner mitochondrial membrane such that the proteins are exposed to the IMS.

During its normal biosynthesis, a heme group is covalently attached to i-cytochrome c_1 in the IMS. This modification is required for the processing of i-cytochrome c_1 to mature cytochrome c_1 (*3, 6*). To assess whether heme is covalently attached to i-cytochrome c_1 accumulating in JN109 mutant cells, we stained mitochondrial proteins isolated from DL2 and JN109 cells after SDS-PAGE with tetramethylbenzidine, a dye that specifically detects heme (*30*). Two prominent bands were stained in each protein fraction (Fig. 4). In the case of mitochondrial protein isolated from DL2 wild-type cells these bands corresponded to cytochrome c and mature cytochrome c_1, both of which contained covalently bound heme (Fig. 4, lane 2). Analysis of mitochondrial protein from JN109 cells indicated that i-cytochrome c_1 also contains covalently bound heme (Fig. 4, lane 1). Both i-cytochrome c_1 and cytochrome c in mitochondria of the mutant strain were stained to a similar degree as the corresponding proteins in mitochondria from the wild-type strain. Thus, the mutation in strain JN109 did not affect heme biosynthesis or the covalent attachment of the heme group to either cytochrome c or i-cytochrome c_1. These data also substantiated the localization of i-cytochrome c_1 to the IMS, because cytochrome c_1 heme lyase, the enzyme catalyzing the covalent heme attachment, is found in this compartment (*31*).

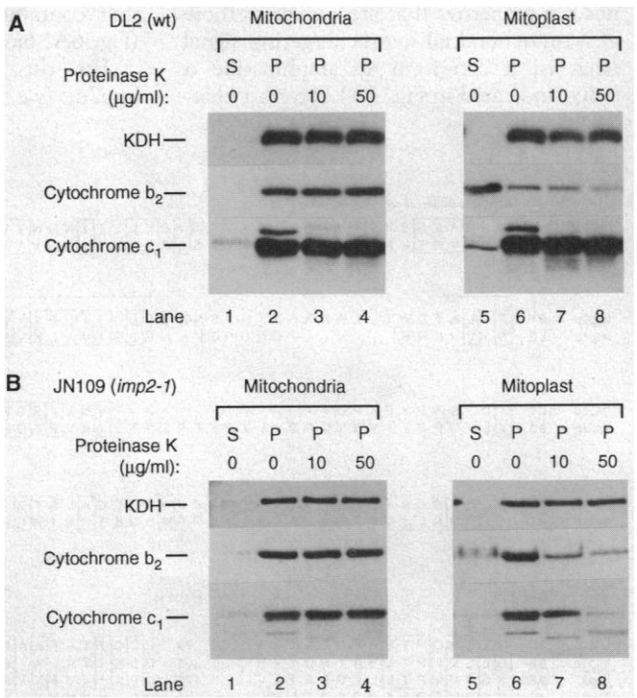

Fig. 3. Intermembrane space exposure of intermediate forms of nuclear-encoded mitochondrial IMS in JN109 cells. Mitochondria were prepared and mitoplasts were formed by osmotic shock as described below. Equivalent amounts of supernatants (S) and mitochondria (P) from mock-treated (0.6 M sorbitol) and osmotically shocked (0.2 or 0.1 M sorbitol) mitochondria (mitoplasts) were analyzed by proteolysis with Proteinase K (0 to 50 μg/ml), SDS-PAGE, and immunoblotting. (**A**) DL2(wt) cells. (**B**) JN109(*imp2-1*) cells. Cultures were grown in YP medium containing 2 percent galactose to log phase at 30°C. Mitochondria were prepared essentially as described (*38*). Cells at 50 A_{600} unit per milliliter were treated with Zymolyase-100T (0.1 mg/ml) (to produce spheroplasts) at 30°C for 1 hour. Cells were lysed by Dounce homogenization on ice (20 strokes) in mitochondrial isolation buffer (MIB) composed of 0.6 M sorbitol, 50 mM Hepes-KOH, pH 7.4, containing the following protease inhibitors: pepstatin A (2 μg/ml), chymostatin (2 μg/ml), antipain (2 μg/ml), and leupeptin (2 μg/ml) and 0.5 mM phenylmethylsulfonylfluoride (PMSF). Unbroken cells and nuclei were removed by centrifugation at 3000*g* for 5 minutes at 4°C. The supernatant of this 3000*g* fraction was centrifuged at 10,000*g* for 10 minutes at 4°C. The pellet from the 10,000*g* centrifugation was washed ten times with MIB containing protease inhibitors. Mitochondria were resuspended at a final protein concentration of 20 mg/ml in MIB containing the protease inhibitors, washed with MIB to remove the inhibitors, and resuspended in MIB at a final protein concentration of 1 mg per milliliter. Mitoplasts were formed by osmotic shock. Sorbitol concentration was reduced to 0.2 M for mitochondria derived from wild-type strain DL2 or to 0.1 M for mitochondria derived from mutant strain JN109 by dilution with 50 mM Hepes, pH 7.4, and incubated on ice for 20 minutes. Mock-treated or osmotically shocked mitochondria were collected by centrifugation and resuspended in MIB at a concentration of 1 mg of protein per milliliter. The resulting samples were then digested with proteinase K. Portions corresponding to 100 μg of mitochondria were treated with proteinase K at concentrations ranging from 10 to 50 μg per milliliter for 30 minutes on ice. After digestion, proteinase K was inactivated by the addition of 1 mM PMSF. Membranes were collected by centrifugation and resuspended in MIB with 1 mM PMSF and treated with trichloroacetic acid at 60°C as described (*13*).

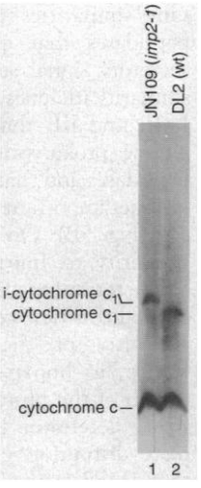

Fig. 4. Covalent attachment of heme to the intermediate form of cytochrome c_1 in JN109 cells. Mitochondria were isolated from the mutant strain JN109 (lane 1) and from the wild-type strain DL2 (lane 2) as described in the legend to Fig. 3. Portions corresponding to 50 μg of protein from both strains were analyzed by SDS-PAGE and stained with tetramethylbenzidine (Sigma) staining (*30*). The mature and intermediate (i) forms of cytochrome c_1 are indicated and were confirmed by immunoblotting.

Taken together, the above data demonstrate that i-cytochrome c_1 and i-cytochrome b_2 accumulate in mutant JN109 cells in a form that is associated with the inner membrane and is exposed to the IMS. We therefore conclude that the mutation in JN109 affects a maturation step of IMS proteins but does not interfere with their proper delivery to the IMS.

Complementation of the mutation in JN109 by a gene encoding a protein related to Imp1p. We cloned and sequenced the defective gene by complementation of the pet$^-$ phenotype with a plasmid from a yeast genomic library in a low-copy vector carrying the *URA* gene (*32*). The *ura3-52* mutation was introduced into the mutant cells by crossing JN109 with wild-type strain PS32.3C and, after sporulation, colonies were isolated that were ura$^-$ pet$^-$ [(*33*); strain JN143]. The DNA from the library was transformed and respiration competent colonies were isolated on plates containing the nonfermentable carbon sources ethanol and glycerol. Two plasmids, containing an identical insert, were isolated. The complementing region was identified by subcloning and sequenced. This analysis revealed an open reading frame that predicted a protein of 177 amino acids (Fig. 5A). A DNA segment comprising only the open reading frame was amplified by PCR (polymerase chain reaction) and, when introduced into JN143 cells, was shown to be sufficient to restore growth on nonfermentable media. These results suggest that the identified open reading frame corresponded to the gene that is defective in the JN143 cells.

A comparison of the sequence with available protein and nucleotide sequence data bases revealed that the open reading frame encoded a previously unidentified protein. The predicted protein closely resembles Imp1p (25 percent amino acid identity; 44 percent amino acid similarity) (Fig. 5A), and, like Imp1p, has more distant similarities to the family of signal peptidases that catalyze the cleavage of secretory signal sequences (Fig. 5B). The similarity includes three regions, designated I, II, and III, that are strongly conserved among prokaryotic and eukaryotic signal peptidases and that may contain amino acid residues important for catalytic activity (*34, 35*) (Fig. 5B). On the basis of the sequence similarity to Imp1p and the biochemical characterization described below, we have termed this new gene *IMP2*. The sequence similarity of the *IMP2* gene product, Imp2p, to Imp1p extends over the entire length of the proteins (Fig. 5A).

To determine the phenotype of a complete disruption of *IMP2* and to confirm that *IMP2* is the gene that is mutated in JN143 cells, we replaced the entire coding sequence of *IMP2* with *LEU2* to generate strain JN174(Δ*imp2*) (*36*). Our results indicated that JN143 and JN174(Δ*imp2*) cells have similar growth and biochemical phenotypes; like JN143 cells, JN174(Δ*imp2*) cells are viable on fermentable medium, but are unable to grow on nonfermentable medium, and accumulate i-cytochrome b_2 and i-cytochrome c_1 as well as pre-COXII. When JN143 cells were crossed to JN174 cells, the resulting diploid strain also was unable to grow on nonfermentable medium, thus providing further support to the likelihood of *IMP2* and the gene mutant in JN143 cells being allelic.

The accumulation of i-cytochrome b_2 and i-cytochrome c_1 in the IMS and the structural similarity of Imp2p to signal peptidases suggested that Imp2p might be directly involved in the processing steps of these proteins. If this were the case, Imp2p should also be localized in mitochondria. Consistent with this possibility, the amino acid sequence of Imp2p at the NH_2-terminus has properties that are similar to those of a mitochondrial matrix targeting signal (that is, it can form an amphipathic α helix, indicated in Fig. 5A). To start characterizing Imp2p biochemically, we inserted a synthetic DNA sequence encoding an epitope from the influenza virus hemagglutinin protein (HA epitope) at the 3′ end of the gene, generating plasmid pIMP2-HA (*37*). When the resulting fusion protein (Imp2p-HA) was expressed from a single copy plasmid (pIMP2-HA) in JN143 and JN174 cells, wild-type growth on nonfermentable medium was observed and the accumulation of i-cytochrome b_2 and i-cytochrome c_1 was suppressed. This indicated that the presence of the HA epitope tag did not impede the function of Imp2p.

Extracts from JN143 cells bearing pIMP2-HA were subjected to SDS-PAGE and subsequent immunoblot analysis. In agreement with the predicted size of the Imp2p-HA fusion protein, a 20-kD band was detected with antibody to HA (anti-HA) in JN143(pIMP2-HA) cell extracts (Fig. 6A, lane 2), but not in extracts derived from JN143 cells bearing a plasmid that contained the wild-type *IMP2* gene (Fig. 6A, lane 1).

For the intracellular localization of Imp2p, we fractionated extracts from

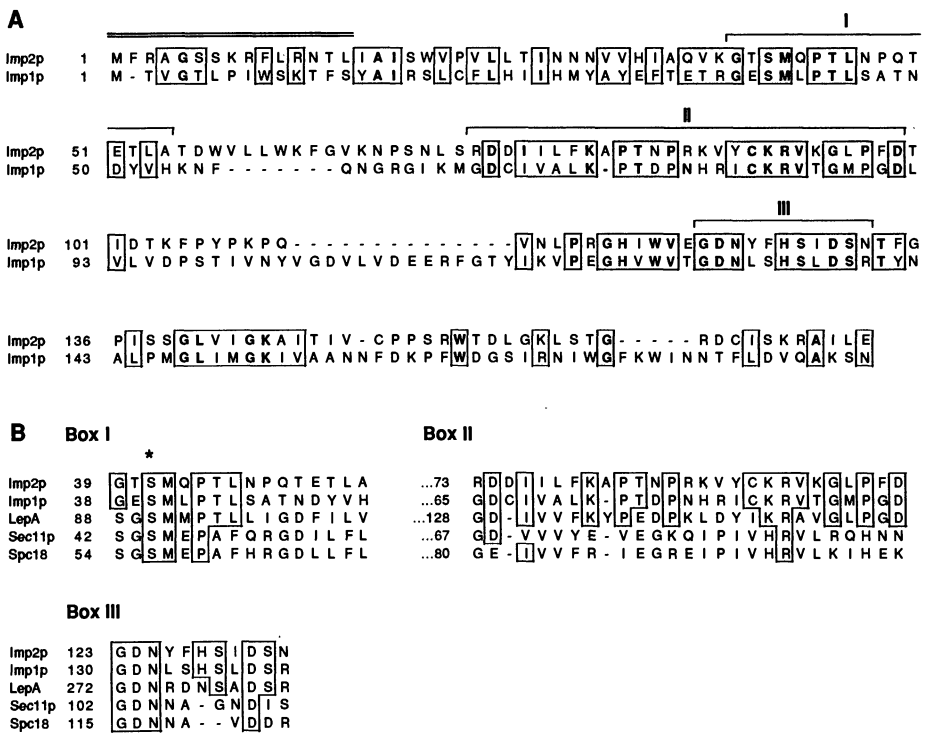

Fig. 5. Primary structure similarity of Imp2p to signal peptidases. (**A**) Sequence alignment of Imp2p and Imp1p (*22*). Bold letters indicate exact matches and boxed letters include both exact matches and conservative changes. The putative matrix targeting signal of Imp2p is indicated by a double line. (**B**) Alignment of the three conserved elements in the signal peptidase family with representative family members and the consensus sequence (*34, 35*). The family members are the following: the *E. coli* leader peptidase, LepA (*53*), the *S. cerevisiae* endoplasmic reticulum (ER) signal peptidase, Sec11p (*54*), and the 18-kD subunit of the canine pancreatic ER signal peptidase, Spc18 (*48*). The putative catalytic serine residue (Ser^{41} in Imp2p) is indicated by an asterisk. Boxed letters indicate exact matches. Abbreviations for the amino acid residues are: A, Ala; C, Cys; D, Asp; E, Glu; F, Phe; G, Gly; H, His; I, Ile; K, Lys; L, Leu; M, Met; N, Asn; P, Pro; Q, Gln; R, Arg; S, Ser; T, Thr; V, Val; W, Trp; and Y, Tyr.

JN143(pIMP2-HA) cells by differential centrifugation (*38*). Samples from each fraction were subjected to SDS-PAGE and immunoblot analysis with anti-HA and an antibody to the mitochondrial matrix protein KDH (Fig. 6B). After low speed centrifugation (3000g) of the extract, a similar fraction of Imp2p-HA and KDH proteins (Fig. 6B, lane 2) were recovered in the pellet, probably because of incomplete cell lysis. When the low-speed supernatant was subjected to greater centrifugal forces (10,000g), both Imp2p-HA and KDH again cofractionated and were quantitatively recovered in the pellet (Fig. 6B, lanes 3 and 4), which is consistent with a mitochondrial localization of both proteins. In addition, Imp2p-HA, like KDH, in the mitochondrial fraction was protected from digestion with proteinase K (Fig. 6C, lanes 2 to 4). Imp2p-HA was recovered in the pellet after the centrifugation procedure used to recover the mitoplasts (Fig. 6C, lane 6). Unlike KDH, Imp2p-HA was rendered protease-sensitive by this treatment (Fig. 6C, compare lane 6 with lanes 7 and 8). Taken together, these results suggest that Imp2p-HA, and—by extention Imp2p—is a mitochondrial inner membrane protein that is exposed to the IMS.

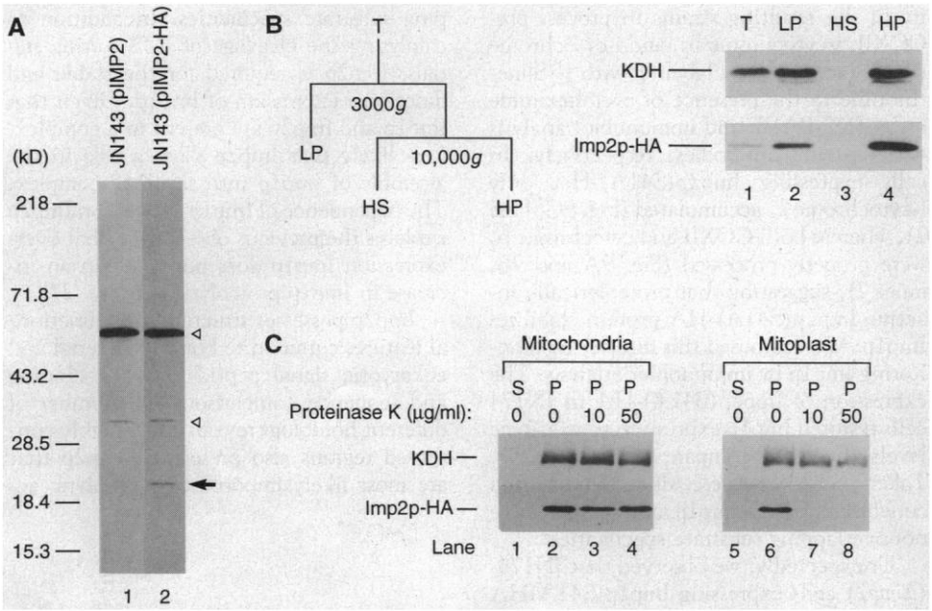

Fig. 6. Mitochondrial localization of Imp2p. Cultures of strain JN143 containing pIMP2-HA (*37*) or pIMP2, were grown in YP containing 2 percent galactose. Cells were spheroplasted, lysed, and fractionated, and mitoplasts were formed from isolated mitochondria as described in the legend to Fig. 3. (**A**) A constant amount (100 μg of protein) of each of the total cell lysate fraction from pIMP2 (lane 1) and pIMP2-HA cells (lane 2) was analyzed by SDS-PAGE and immunoblotting with monoclonal anti-HA (ascites fluid 12CA-4; lot E, BAbCO). The arrow indicates Imp2p and the triangles indicate proteins that crossreacted with the anti-HA and were observed in extracts of cells that were not expressing pIMP2-HA. (**B**) A constant amount (100 μg of protein) of each of the total cell lysate fraction from pIMP2-HA cells (T, lane 1), the 3000*g* pellet (LP, lane 2), the 10,000*g* supernatant (HS, lane 3), and the 10,000*g* pellet fraction (HP, lane 4) was analyzed by SDS-PAGE and immunoblotting with antibody to HA or with antibodies directed against the mitochondrial matrix marker KDH. (**C**) Equivalent amounts of supernatants (S) and mitochondria (P) from mock-treated (0.6 M sorbitol) and osmotically shocked (0.2 M sorbitol) mitochondria were analyzed by proteolysis with proteinase K (0 to 60 μg/ml), SDS-PAGE, and immunoblotting with the indicated antibodies.

Imp2p-HA, and—by extention Imp2p—is a mitochondrial inner membrane protein that is exposed to the IMS.

Nonoverlapping substrate specificities of Imp1p and Imp2p. On the basis of their primary structure similarity, Imp2p and Imp1p may both be proteases that catalyze the cleavage of IMS targeting signals. This interpretation poses, however, the following paradox. Depending on the phenotypes of the mutants, both *IMP1* and *IMP2* are required for the processing of pre-COXII and i-cytochrome b_2 whereas only mutations in *IMP2* block the processing of i-cytochrome c_1. Thus, *imp2* mutants elicit a broader spectrum of processing defects including those resulting from mutations in *IMP1*. One resolution for this puzzle is that Imp1p and Imp2p may have different, nonoverlapping substrate specificities (Imp1p processing pre-COXII and i-cytochrome b_2 and Imp2p processing i-cytochrome c_1), but that Imp2p may be required for the function of Imp1p.

To test this possibility, we determined the Imp1p content of JN174(Δ*imp2*) cells. The JN174(Δ*imp2*) and wild-type control cell extracts were fractionated as before by differential centrifugation, and Imp1p and KDH were detected by immunoblotting with specific antibodies after SDS-PAGE (Fig. 7A). In contrast to wild-type cells (Fig. 7A, lanes 1 to 3), the amount of Imp1p in JN174(Δ*imp2*) cells was dramatically reduced (Fig. 8A, lanes 4 to 6), whereas the amount of KDH was unchanged. RNA (Northern) blot analysis of RNA derived from JN174(Δ*imp2*) cells showed that the amount of *IMP1* mRNA in the mutant cells was indistinguishable from that in wild-type cells (Fig. 7B), suggesting that Imp1p was synthesized in comparable amounts in wild-type and *imp2* mutant cells, but was unstable in the mutant cells.

It is possible that Imp2p functions to stabilize Imp1p by forming a complex with Imp1p in the mitochondrial inner membrane. We tested this possibility directly by immunoprecipitation with anti-HA from a nondenaturing detergent extract of mitochondria derived from JN143(pIMP2-HA) cells. Immunoprecipitated proteins were subjected to SDS-PAGE and subsequent immunoblot analysis. Imp2p-HA was pre-

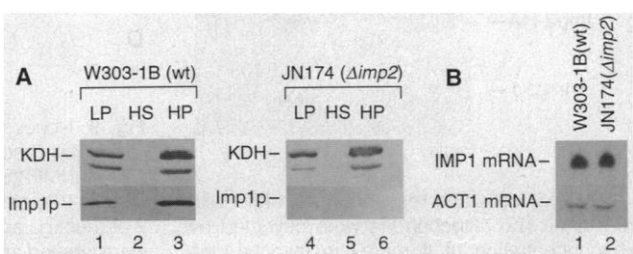

Fig. 7. Requirement of Imp2p for the assembly of Imp1p in the mitochondria (**A**) Cultures of strain JN174 were grown in YP containing 2 percent galactose. Cells were spheroplasted, lysed, and fractionated as described in the legend to Fig. 3. A constant amount (100 μg of protein) of each of the 3000*g* pellet (LP, lane 1 and 4), the 10,000*g* supernatant (HS, lane 2 and 5) and the 10,000*g* pellet (HP, lane 3 and 6) was analyzed by SDS-PAGE and immunoblotting with antibody to Imp1p or to the mitochondrial marker KDH. (**B**) Cultures of JN174 and W303-1B were grown in YP containing 2 percent galactose. RNA was prepared from these cultures (*55*). Portions corresponding to 30 μg of RNA were subjected to electrophoresis on a 1.4 percent agarose gel containing formaldehyde. RNA was transferred to Hybond-N (Amersham) nylon membrane by capillary action and crosslinked to the membrane by ultraviolet irradiation. Blotted *IMP1* and *ACT1* mRNA was detected by labeling the full-length *IMP1* gene (*22*) and a 140-bp fragment of the *ACT1* gene (*56*) by random priming with [α-^{32}P]dCTP. IMP1 and ACT1 probes were hybridized overnight to the total RNA blot at 65°C in 7 percent SDS, 0.5 M sodium phosphate buffer, pH 7.0, and 2 mM EDTA. The blot was washed three times for 15 minutes at 65°C in 2 percent SDS, 0.15 M sodium phosphate buffer, pH 7.0, and 2 mM EDTA (*57*).

cipitated from the mitochondrial extract (Fig. 8, lanes 2 and 4). In particular, Imp1p (detected with antibodies to Imp1p) was co-immunoprecipitated by the anti-HA from the mitochondrial extracts. The immunoprecipitation of both Imp2p-HA and Imp1p was blocked by the addition of excess peptide corresponding to the HA epitope (Fig. 8, lanes 1 and 3), indicating that the co-immunoprecipitation of Imp1p with Imp2p-HA was specific. The fraction of Imp1p precipitated with anti-HA was less than that observed for Imp2p; however, when analyzed by velocity sucrose gradient sedimentation, Imp1p and Imp2p-HA cofractionated quantitatively. We conclude that Imp1p and Imp2p-HA—and by extention Imp1p and Imp2p—are associated in a protein complex, that is, however, partially destabilized under the immunoprecipitation conditions.

The above data suggest that (i) Imp2p is the protease required for processing of i-cytochrome c_1 and (ii) that it is required for the stable expression of Imp1p, which in turn is the protease required for the processing of pre-COXII and i-cytochrome b_2. To test directly whether Imp2p and Imp1p have nonoverlapping substrate specificities, we used site-directed mutagenesis to inactivate specifically the proteolytic activity of Imp2p (*39*). A specific mutation would leave Imp2p structurally intact and still enable the inactive Imp2p to assemble into a complex with Imp1p thereby stabilizing Imp1p in the inner membrane. Therefore, we changed Ser^{41} in Imp2p-HA to alanine, generating plasmid pIMP2(S41A)-HA. Serine-41 is likely to be part of the active sites of the family of signal peptidases; it occurs in the conserved sequence region I of all eukarytoic and prokaryotic signal peptidases (Fig. 5B) (*34, 35*), and point mutants in the corresponding residue in *Escherichia coli* leader peptidase have been shown to inactivate the enzyme (*40*).

To examine the effects of the S41A mutation, the plasmids pIMP2(S41A)-HA or pIMP2-HA (as a control) were transformed into JN174(Δ*imp2*) cells. The ability of the resulting strains to process pre-COXII, i-cytochrome b_2, and i-cytochrome c_1 was monitored by labeling with [^{35}S]methionine in the presence of cycloheximide or by SDS-PAGE and immunoblot analysis with specific antibodies, respectively. In cells expressing Imp2p(S41A)-HA only i-cytochrome c_1 accumulated (Fig. 9C, lane 2), whereas both COXII and cytochrome b_2 were properly processed (Fig. 9A and 9B, lanes 2), suggesting that proteolytically inactive Imp2p(S41A)-HA protein stabilizes Imp1p. We examined this directly by monitoring Imp1p by immunoblot analysis. The expression of Imp2p(S41A)-HA in JN174 cells restored Imp1p expression to wild-type levels (Fig. 9D, compare lanes 2 and 3). Taken together these data demonstrate conclusively that Imp1p and Imp2p have nonoverlapping substrate specificities.

Unexpectedly, we observed that JN174-(Δ*imp2*) cells expressing Imp2p(S41A)HA are no longer pet$^-$ and grow with wild-type rates on nonfermentable medium. This observation implies that the bc_1 complex is functional, that is, that the accumulated i-cytochrome c_1—although not properly assembled as judged by its protease sensitivity in mitoplasts (Fig. 3B, lanes 7 and 8)—may be active.

Relation of inner membrane protease to the signal peptidase family. We have identified a novel *S. cerevisiae* gene product, Imp2p, and propose that it is a catalytic component of mitochondrial inner membrane protease (IMP), a protease responsible for the maturation of mitochondrial IMS proteins. We have shown that IMP is a complex composed of at least two nonidentical, but structurally similar subunits, Imp1p and Imp2p, that have nonoverlapping substrate specificities. In addition to catalyzing the cleavage of IMS sorting signals, Imp2p is required for the stable and functional expression of Imp1p. Given that Imp1p and Imp2p are present in a complex, it is likely that Imp2p plays a role in the assembly of Imp1p into the IMP complex. The dependence of Imp1p activity on Imp2p explains the previous observation that overexpression Imp1p does not result in an increase in Imp1p proteolytic activity (*21*).

Imp2p possesses structural and functional features common to both eubacterial and eukaryotic signal peptidases. The cloning and sequence comparison of a number of different homologs reveals three highly conserved regions also present in Imp2p that are most likely important for catalytic ac-

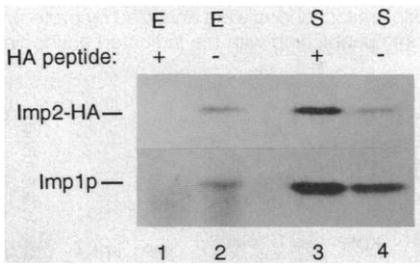

Fig. 8. Imp2p and Imp1p as part of a complex. Mitochondria were prepared and solubilized as described in legend to Fig. 3 and below. Solubilized mitochondria were immunoprecipitated with anti-HA in the presence (lanes 1 and 3) or absence (lanes 2 and 4) of excess HA peptide. Supernatant fractions (S, lanes 3 and 4) and protein A–Sepharose eluate fractions (E, lanes 1 and 2) were analyzed by SDS-PAGE and immunoblotting with anti-HA and anti-Imp1p. The fraction of Imp2p-HA that was immunoprecipitated with anti-HA varied between 20 to 100 percent. Mitochondria were isolated from JN174(Δ*imp2*) cells and resuspended in MIB with protease inhibitors at a protein concentration of 20 mg/ml. The mitochondria were collected by centrifugation and resuspended at a final protein concentration of 4 mg/ml in mitochondria resuspension buffer (MRB), containing 20 mM tris-HCl, pH 7.5, 20 mM $MgCl_2$, 20 percent glycerol and protease inhibitors, with the addition of 200 mM KCl. Mitochondria were solubilized by the addition of an equal volume of MRB containing 6 percent MEGA-8 (CalBiochem) followed by incubation for 15 minutes on ice. Samples were centrifuged at 100,000*g* for 20 minutes. The resulting supernatant was first adsorbed to a 0.25 volume of Sepharose CL-4B (Pharmacia) by mixing at 4°C for 15 minutes. The Sepharose beads were removed by centrifugation. Anti-HA (1 μl) was either diluted in 50 μl of MRB containing 100 mM KCl and 3 percent MEGA-8 (MRB+) or in 50 μl of MRB+ containing 50 μg of HA peptide (NH_2-YPYDVPDYA-COOH) and then incubated on ice for 15 minutes. Antibody was mixed with portions of mitochondrial supernatant (200 μl) and incubated on ice for 1 hour. A 20-μl portion of protein A Sepharose CL-4B (Sigma) was added and mixed at 4°C for 20 minutes. The protein A–Sepharose beads were centrifuged, washed five times with MSB+, and analyzed by SDS-PAGE and immunoblotting.

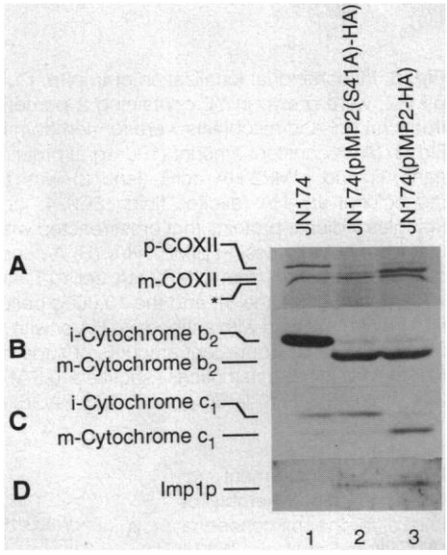

Fig. 9. Nonoverlapping substrate specificities of Imp2p and Imp1p. Cultures of JN174, JN174(pIMP2(S41A)-HA) (*39*), and JN174 (pIMP2-HA) cells were grown in YP containing 2 percent galactose. (**A**) Mitochondrial proteins were labeled and analyzed as described in Fig. 1. As in Fig. 1, incorporation of [^{35}S]methionine into mitochondrial translation products was variable between experiments. The asterisk indicates the mitochondrial translation product cytochrome b. (**B**, **C**, and **D**) Total extract (100 μg) was prepared and immunoblotted with the indicated antibodies as described in Fig. 3. (A) The COXII precursor (p-COXII) and mature COXII (m-COXII) are indicated. The mature and intermediate forms of cytochrome b_2 (B) and cytochrome c_1 (*58*) (C) are indicated. The gel was blotted with antibodies to Imp1p (D).

tivity (Fig. 5B) (*34, 35*). The mechanism of signal peptidase-catalyzed peptide bond cleavage, however, remains unknown. In particular, there are no known inhibitors of this class of proteases and, hence, the chemical nature of the reactive groups involved in catalysis remain uncharacterized (*42*). A serine residue in sequence region I is found in all members of this family and is essential for the proteolytic activity of *E. coli* leader peptidase (*34, 35, 40*). Thus, it has been proposed that the proteases belonging to this family are serine proteases. Consistent with this idea, our data show that the corresponding serine residue in Imp2p, Ser^{41}, is essential for the proteolytic activity of Imp2p. Unlike conventional serine proteases, however, proteases of the signal peptidase family lack a conserved histidine residue (essential to activate the catalytic serine) and, thus, constitute a distinct class of proteases (*35, 41*).

Our results indicate that Imp2p is a mitochondrial inner membrane–associated protein with a large domain located in the IMS. Adjacent to the putative mitochondrial matrix targeting sequence composed of the 14 NH_2-terminal residues (Fig. 5A) is a stretch of hydrophobic amino acids (residues 15 to 27) that is likely to be important for the observed inner membrane association. The remainder of the Imp2p polypeptide, including the conserved regions implied in catalysis, is located in the IMS, as deduced from the accessibility of the COOH-terminus to proteolysis (Fig. 6C). Thus, in addition to primary structure homology, Imp2p has a similar topology to both the eubacterial and eukaryotic signal peptidases, which are membrane-associated enzymes with their active sites facing the compartment to which the substrate molecules become localized during their biogenesis (*42, 43*).

The multisubunit structure of IMP distinguishes it from the single subunit eubacterial signal peptidases, although—consistent with the endosymbiont theory which proposes that mitochondria have evolved from eubacterial origins—both Imp1p and Imp2p show the closest primary structure similarity to the eubacterial enzymes (Fig. 5B). The multisubunit structure is a characteristic found in eukaryotic signal peptidases (*44–46*). The well-characterized canine pancreatic peptidase, for example, is a complex of five non-identical polypeptides; similar to IMP, two of these subunits are related to each other and to eubacterial peptidases and, thus, are likely to be the catalytic subunits (*44, 47–49*).

The significance of multiple catalytic subunits in the eukaryotic signal peptidase complex is unknown; however, a possible answer to this question may be provided by our observation that Imp1p and Imp2p have nonoverlapping substrate specificities. Indeed, examination of the cleavage sites of the different pre-protein substrates indicates that their structures can be distinguished. The Imp2p-dependent substrate, i-cytochrome c_1, contains a cleavage site similar to most of the known substrates of eubacterial and eukaryotic peptidases in which small amino acids are present at the −1 and −3 positions (Ala and Ser, respectively). In contrast, the Imp1p-dependent substrates, pre-COXII and i-cytochrome b_2, both contain a large asparagine residue at the −1 position and, thus, deviate considerably from the standard motif. Similarly, eukaryotic signal peptidase has been proposed to cleave some substrates at nonstandard cleavage sites (*50*). Given this, we propose that during evolution IMP, and by analogy eukaryotic multisubunit signal peptidases, have acquired multiple catalytic subunits by gene duplication which allowed them to broaden their range of substrate specificity. It is possible that the organization of multiple catalytic subunits in a complex allows for their colocalization to the protein translocation sites where their substrates emerge into the intermembrane space.

REFERENCES AND NOTES

1. I. Sadler, K. Suda, G. Schatz, F. Kaudewitz, A. Haid, *EMBO J.* **3**, 2137 (1984).
2. B. Guiard, *ibid.* **4**, 3265 (1985).
3. A. Ohashi, J. Gibson, I. Gregor, G. Schatz, *J. Biol. Chem.* **257**, 13042 (1982).
4. G. A. Reid, T. Yonetani, G. Schatz, *ibid.*, p. 13068.
5. S. M. Gasser *et al.*, *Proc. Natl. Acad. Sci. U.S.A.* **9**, 267 (1982).
6. D. W. Nicholson, R. A. Stuart, W. Neupert, *J. Biol. Chem.* **264**, 10156 (1989).
7. C. Witte, R. E. Jensen, M. P. Yaffe, G. Schatz, *EMBO J.* **7**, 1439 (1988).
8. R. E. Jensen and M. P. Yaffe, *ibid.*, p. 3863.
9. M. Yang, R. E. Jensen, M. P. Yaffe, W. Oppliger, G. Schatz, *ibid.*, p. 3857.
10. A. P. G. M. van Loon, A. W. Brändli, G. Schatz, *Cell* **44**, 801 (1986).
11. A. P. G. M. van Loon, A. W. Brändli, B. Pesold-Hurt, D. Blank, G. Schatz, *EMBO J.* **6**, 2433 (1987).
12. M. Nguyen, A. W. Bell, G. C. Shore, *J. Cell Biol.* **106**, 1499 (1988).
13. B. S. Glick *et al.*, *Cell* **69** (1992).
14. F.-U. Hartl and W. Neupert, *Science* **247**, 930 (1990).
15. F.-U. Hartl, J. Ostermann, B. Guiard, W. Neupert, *Cell* **51**, 1027 (1987).
16. H. Koll *et al.*, *ibid.* **68**, 1163 (1992).
17. G. H. D. Clarkson and R. O. Poyton, *J. Biol. Chem.* **264**, 10114 (1989).
18. K. A. Severino and R. O. Poyton, *Proc. Natl. Acad. Sci. U.S.A.* **77**, 142 (1980).
19. E. Pratje, G. Mannhaupt, G. Michaelis, K. Beyreuther, *EMBO J.* **2**, 1049 (1983).
20. E. Pratje and B. Guiard, *ibid.* **5**, 1313 (1986).
21. A. Schneider *et al.*, *ibid.* **10**, 247 (1991).
22. M. Behrens, G. Michaelis, E. Pratje, *Mol. Gen. Genet.* **228**, 167 (1991).
23. E. Schwarz, T. Seytter, B. Guiard, W. Neupert, *EMBO J.* **12**, 2295 (1993).
24. E. M. Beasley, S. Muller, G. Schatz, *ibid.* p. 2303.
25. M. C. Costanzo, E. C. Seaver, T. D. Fox, *ibid.* **5**, 3637 (1986).
26. L. S. Folley and T. D. Fox, *Genetics* **129**, 659 (1991).
27. J. J. Mulero and T. D. Fox, *Mol. Gen. Genet.*, in press.
28. S. Wakabayashi, H. Matsubara, C. H. Kim, K. Kawa, T. E. Kng, *Biochem. Biophys. Res. Commun.* **97**, 1548 (1980).
29. M. Crivellone, M. Wu, A. Tzagoloff, *J. Biol. Chem.* **263**, 14323 (1988).
30. P. E. Thomas, D. Ryan, W. Levin, *Anal. Biochem.* **75**, 168 (1976).
31. A. Zollner, G. Rödel, A. Haid, *Eur. J. Biochem.* **207**, 1093 (1992).
32. M. Rose, P. Novick, J. Thomas, D. Botstein, G. Fink, *Gene* **60**, 237 (1987).
33. Strain JN109 was backcrossed to wild-type strain PS32.3C and sporulated. Tetrads were dissected and analyzed for both pet^- and ura^- phenotype. One meiotic product that was both pet^- and ura^- (strain JN143) was transformed with a centromeric YCp50-based yeast genomic library containing inserts of 10 to 15 kb (average) (*32*), and ura^+ colonies were replica-plated onto YP plates containing ethanol and glycerol as carbon sources (YPEG). Two independent transformants (total of 10,000) displayed plasmid-dependent growth on YPEG. The plasmids were isolated by bead beating in the presence of phenol, and the isolated DNA was purified (Magic Mini-Prep; Promega). Restriction mapping showed that both plasmids contained an identical insert. The minimal size of insert DNA capable of supporting growth on YPEG was determined by a partial Sau 3A digestion of the complementing plasmid. The average Sau 3A DNA fragment length was 3 to 4 kb. These fragments were cloned into the Bam HI site of pRS316 (*59*) and retransformed into strain JN109. Double-stranded sequencing of both strands of a 3-kb piece of complementing insert DNA was performed by the dideoxy nucleotide chain termination method with Sequenase (version 2.0, U.S. Biochemicals) and synthetic DNA primers. The complementing ORF was confirmed by PCR amplification and, when transformed into mutant JN143 cells, restored growth on nonfermentable carbon sources and suppressed the processing defect. The Genbank accession number of the IMP2 sequence is L26340.
34. J. Maarten van Dijl, A. de Jong, J. Vehmaanperä, G. Venema, S. Bron, *EMBO J.* 11, 2819 (1992).
35. R. E. Dalbey and G. von Heijne, *Trends Biochem. Sci.* **17**, 474 (1992).
36. The null phenotype of *IMP2* was assessed by replacing the entire coding sequence of *IMP2* with *LEU2* in the chromosome (strain JN174). The genomic upstream and downstream flanking regions of *IMP2* were generated using the PCR. A 216-bp upstream fragment with a 5′ Bam HI site and a 3′ Sma I site (corresponding to nucleotides −3 to −219; numbered from AUG) and a 200-bp downstream fragment with 5′ Sma I site and a 3′ Eco RI site (corresponding to 552 to 752) were amplified and cloned into pRS316 (*URA*/CEN) (*59*) in a three piece ligation to yield plasmid pJN127. A 2.2-kb Sal I fragment containing the *LEU2* gene, derived from pLSK1 (gift of J. Lee, UCSF) was blunted with T4 polymerase and cloned into the Sma I site of pJN127 to yield pJN128. The 2.6-bp Bam HI–Eco RI fragment from pJN128 was used to transform the haploid strains W303-1B and transformants were selected by plating cells on −Leu plates. The disruption in strain JN174 was confirmed by PCR of genomic DNA derived from JN174.
37. A 5′ Bam HI site (at nucleotide −219) and an in-frame 3′ Nco I site (at nucleotide 530, replacing the stop codon) was introduced by PCR into *IMP2*. A 460-bp fragment derived from pSF19 (gift of P. Sorger, MIT) containing DNA encoding the amino acids of the HA peptide and the actin terminator region was ligated to the 750-bp Bam HI–Nco I *IMP2* fragment in pRS316 (*59*). The resulting plasmid pJN104 encoding an HA-tagged Imp2p was transformed into strain JN143.
38. G. Daum, P. C. Böhni, G. Schatz, *J. Biol. Chem.* **257**, 13028 (1982).
39. Site-directed mutagenesis was performed with the Mutagene kit (Bio-Rad). The DNA oligonucle-

otide used for mutagenesis was 5′-GCA AGT TAA AGG TAC AGC TAT GCA GCC TAC G-3′.
40. N. Bilgin, J. I. Lee, H.-y. Zhu, R. Dalbey, G. von Heijne, *EMBO J.* **9**, 2717 (1990).
41. M. T. Black, J. G. R. Munn, A. E. Allsop, *Biomed. J.* **282**, 539 (1992).
42. J. L. San Millan, D. Boyd, R. Dalbey, W. Wickner, J. Beckwith, *J. Bacteriol.* **171**, 5536 (1989).
43. G. S. Shelness, L. Lin, C. V. Nicchitta, *J. Biol. Chem.* **268**, 5201 (1993).
44. E. A. Evans, R. Gilmore, G. Blobel, *J. Cell Biol.* **83**, 581 (1986).
45. R. K. Baker and M. O. Lively, *Biochemistry* **26**, 8561 (1987).
46. J. T. YaDeau, C. Klein, G. Blobel, *Proc. Natl. Acad. Sci. U.S.A.* **88**, 517 (1991).
47. E. A. Evans, G. S. Shelness, G. Blobel, *J. Biol. Chem.* **103**, 291 (1986).
48. G. Greenburg, G. S. Shelness, G. Blobel, *ibid.* **264**, 15762 (1989).
49. G. Shelness and G. Blobel, *ibid.* **265**, 9512 (1990).
50. G. Hortin and I. Boime, *Cell* **24**, 453 (1981).
51. Media and general methods. YP and minimal media were prepared as described (*60*). Cells were grown in YP medium containing 2 percent galactose (YP contained galactose in place of glucose to avoid glucose repression of synthesis of mitochondrial proteins), or 2 percent ethanol and 2 percent glycerol (YPEG) as carbon sources. The SDS-PAGE analyses were performed on 10 to 15 percent polyacrylamide gels. Immunological detection of proteins after immunoblotting was performed by enhanced chemiluminesence (Amersham).
52. B. C. Hann and P. Walter, *Cell* **67**, 131 (1991).
53. P. B. Wolfe, W. Wickner, J. M. Goodman, *J. Biol. Chem.* **258**, 12073 (1983).
54. P. Bohni, R. J. Deshaies, R. Schekman, *J. Cell Biol.* **106**, 1035 (1988).
55. K. Kohrer and H. Domdey, *Methods Enzymol.* **194**, 398 (1991).
56. J. S. Cox, C. E. Shamu, P. Walter, *Cell* **73**, 1197 (1993).
57. G. M. Church and W. Gilbert, *Proc. Natl. Acad. Sci., U.S.A.* **81**, 1991 (1984).
58. A minor band present in mitochondria derived from JN174(*Δimp2*) and JN174[pIMP2(S42A)-HA] cells that co-migrates with mature cytochrome c_1 is likely nonspecifically detected by the antiserum cytochrome c_1 used in these studies. We cannot rule out the possibility that the band represents a small amount of i-cytochrome c_1 that has been proteolyzed by other proteases. It is unlikely, however, that this form accounts for the PET$^+$ phenotype of JN174[pIMP2(S42A)-HA] cells, because a similar amount is present in JN174(*Δimp2*) cells which are pet$^-$.
59. R. S. Sikorski and P. Hieter, *Genetics* **122**, 19 (1989).
60. F. Sherman, J. B. Hicks, G. R. Fink, *Methods in Yeast Genetics* (Cold Spring Harbor Laboratory, Cold Spring Harbor, NY, 1986).
61. T. Stearns, Stanford University.
62. R. Rothstein, Columbia University.
63. The following reagents were provided as follows: antibodies to $F_1\beta$-ATPase (M. P. Yaffe, Department of Biology, University of California, San Diego), antibodies to cytochrome b_2 and cytochrome c_1 (W. Neupert, University of Munich, Munich), antibodies to α-ketoglutarate dehydrogenase, to Imp1p, and to cytochrome c (G. Schatz, Biocenter, Basel).
64. We thank R. Fletterick, T. Powers, C. Shamu, and K. Yamamoto for comments on the manuscript. Supported by a postdoctoral fellowship from the American Heart Association (J.N.); an NIH grant (T.D.F.), and grants from the University of California Academic Senate, the Alfred P. Sloan Foundation and NIH (P.W.).

20 August 1993; accepted 15 November 1993